2008

Severe plastic deformation of an as-cast hypoeutectic Al-Si alloy

Swaminathan, S.; Garcia-Infanta, J.M.; McNelley, T.R.; Ruano, O.A.; Carreño, F.

Springer

S. Swaminathan, J.M. Garcia-Infanta, T.R. McNelley, O.A. Ruanon F. Carreño, Sever plastic deformation of an as-cast hypoeutectic Al-Si alloy," Journal of Materials Science, V. 43, (2008), pp. 7501-7506.
http://hdl.handle.net/10945/55334

J Mater Sci (2008) 43:7501–7506
DOI 10.1007/s10853-008-2625-y

ULTRAFINE-GRAINED MATERIALS

Severe plastic deformation of an as-cast hypoeutectic Al–Si alloy

S. Swaminathan · J. M. García-Infanta · T. R. McNelley · O. A. Ruano · F. Carreño

Received: 7 March 2008 / Accepted: 28 March 2008 / Published online: 26 July 2008

Abstract Different equal channel angular pressing (ECAP) processing routes have been employed to investigate the flow plane microstructures in a hypoeutectic Al–7wt%Si. In the as-cast condition, this alloy exhibits equiaxed primary aluminum dendrite cells embedded in an Al–Si eutectic constituent. The observed microstructures have been compared to the predicted distortion of a volume element expected during idealized ECAP. The effect of different processing routes on the microstructure refinement, degree of homogenization of second phase particles, and associated mechanical properties are discussed.

Introduction

Over the past two decades, severe plastic deformation (SPD) processing by equal channel angular pressing (ECAP) [1] has been studied intensively as a potential means for producing bulk ultra-fine grained or nanostructured materials. In ECAP, a billet having a square or circular cross-section is pressed through a die having two channels of equal inlet and outlet areas, and with the channels inclined at an angle with respect to each other. The billet undergoes shear deformation at the die channel intersection, and the strain imposed in a single pass depends on the angle between the channels, radius of curvature at the outer corner of the die channel intersection, and the friction conditions prevailing between the die and billet [2]. Since the billet cross-sectional area does not change during a pass through the die, repetitive pressing operations may be performed on it thereby resulting in large cumulative strains. After N passes, the idealized total strain experienced in the volume of the billet, γ_T, is $2N\cot(\varphi)$, where φ is the shear plane angle (Fig. 1).

The strain path can be varied by the extent and sense of rotation of the billet between passes in repetitive ECAP, which has led to designations of the distinct paths, or routes, as A, B_A, B_C, and C [3, 4]. Routes A and B_A involve a monotonic increase in strain during a succession of passes, while routes B_C and C may involve redundant straining during repetitive ECAP. Route B_C has been cited as most advantageous for achieving microstructure refinement in the fewest passes for pure metals and dilute alloys when pressing is conducted with a die having a 90° die channel angle [5]. However, route A has been suggested as more advantageous for a die channel angle of 120° [6]. Prior grain boundaries generally become indistinguishable beyond the second or third pass in repetitive ECAP irrespective of the processing route for pure metals and dilute alloys, and so, the congruence between expected shape change and microstructure for the various routes has not been clearly illustrated in such materials.

It is possible that a non-deforming second phase may provide a marker to delineate the microstructural shape change during repetitive ECAP and thereby aid in establishing the congruence between the observed and expected shape change for routes involving different strain paths. In turn, this may also shed light on the mechanism(s) of microstructure refinement, degree of

S. Swaminathan · T. R. McNelley (✉)
Department of Mechanical & Astronautical Engineering, Naval Postgraduate School, 700 Dyer Road, Monterey, CA 93943-5146, USA
e-mail: tmcnelley@nps.edu

J. M. García-Infanta · O. A. Ruano · F. Carreño
Department of Physical Metallurgy, Centro Nacional de Investigaciones Metalúrgicas (CENIM), CSIC, Av. de Gregorio del Amo 8, 28040 Madrid, Spain

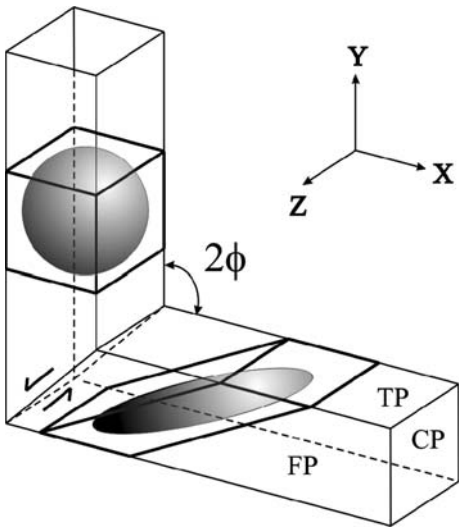

Fig. 1 Schematic of equal channel angular pressing (ECAP) operation showing the distortion of a cubical volume element enclosing a spherical volume element at the die-channel intersection. The reference axes used in this study is also shown

homogenization of particle distributions, and factors influencing mechanical properties. Such a hypothesis forms the basis for this paper wherein large-strain deformation characteristics of a hypoeutectic Al–7wt%Si alloy have been investigated.

Experimental procedure

The Al–7wt%Si alloy was prepared by melting pure Al (99.99 wt%) and Al–12.3wt%Si master alloys along with 0.02 wt% Na addition, resulting in a solidification microstructure consisting of primary aluminum and a refined eutectic constituent containing mainly Si particles. The chemical analysis of the solidified materials as measured by emission spectroscopy was (in wt%) 7.0% Si, 0.3% Fe, and balance Al. The as-cast material was subjected to ECAP processing by routes A, B_A, B_C, and C at room temperature using a sharp-cornered 90° ECAP die (zero die-relief angle at the outer corner of the die channel intersection). The pressing speed used was 10 mm/min.

An idealization of the distortion of a cubical element enclosing a spherical volume element as it is sheared at the die channel intersection is illustrated in Fig. 1 along with the reference axes used in this work. The pertinent plane of interest in this study is the flow plane (FP), i.e., the *X*–*Y* plane, after the end of the pressing operation. As-pressed billets were carefully sectioned to reveal the billet midplane for FP microstructure after 1, 2, 4, and 8 passes with the aid of either optical and/or scanning electron microscopy. Care was taken to characterize samples close to the center of each surface to avoid effects of die-wall friction and dead zone formation at the outer corner of the die channel intersection. For OM observations, the surfaces were metallographically prepared by polishing with a series of abrasives concluding with a 0.05 μm colloidal silica suspension. For SEM analysis, samples were electropolished after metallographic polishing using a solution of 20 vol%$HNOB_{3B}$ + 80 vol%$CHB_{3B}OH$ at −28 °C and 17 V. Backscattered electron (BSE) images were obtained utilizing a field-emission gun scanning electron microscope (FEG-SEM) operating at 10 kV. The microstructures were correlated to the tensile properties reported in an earlier work [7].

Results and discussion

Figure 2 shows both lower- and higher-magnification optical images of the as-cast Al–7wt%Si illustrating equiaxed primary Al dendrite cells along with an eutectic constituent consisting of grey-colored needle-like particles of Al_5FeSi and dark irregular particles of Si in the Al matrix. The primary Al dendrite cell size varies from 25 to 65 μm due to the difference in solidification rates at different locations in the as-cast ingot [8]. The optical microstructure of Al–7wt%Si in the *X*–*Y* plane (i.e., the flow plane) after ECAP processing by different routes is shown in Fig. 3a. After one pass, the microstructure has experienced shear and the primary Al dendrite cells have become elongated such that their long axis is inclined at an angle of ∼22° with the *X*-direction (i.e., the die channel exit direction). The microstructure becomes progressively elongated on pressing by route A (no rotation between successive passes resulting in monotonic shearing), with the long axis of the dendritic cells inclined at angles of ∼14 and ∼7° after two and four passes, respectively. When route B_A (alternating +90 and −90° rotations upon the second and subsequent passes, also resulting in monotonic shearing) is employed, the microstructure after two passes is similar to that after one pass, while the microstructure after four passes resembles that of two passes by route A.

After processing by route B_C (rotations of 90° in the same sense upon the second and subsequent passes, resulting in redundant straining after every fourth pass), the microstructure after two passes resembles that of one pass microstructure, but after four passes, the microstructure is made up of equiaxed primary Al dendritic cells akin to the as-cast microstructure. In the case of processing by route C (rotations of 180° upon the second and subsequent passes, resulting in redundant straining after every other pass), the microstructures after two and four passes are similar to that of the as-cast microstructure and consist of equiaxed primary Al dendritic cells.

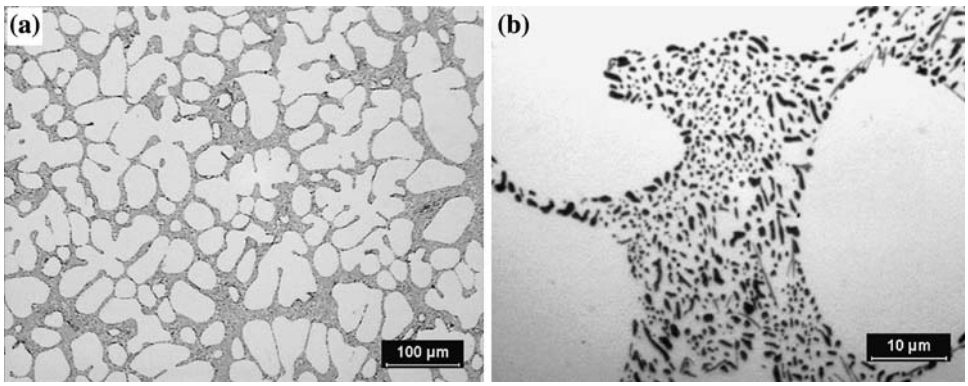

Fig. 2 (**a**) Lower- and (**b**) higher-magnification optical microscopy images of an as-cast microstructure showing primary Al dendritic cells and eutectic constituent

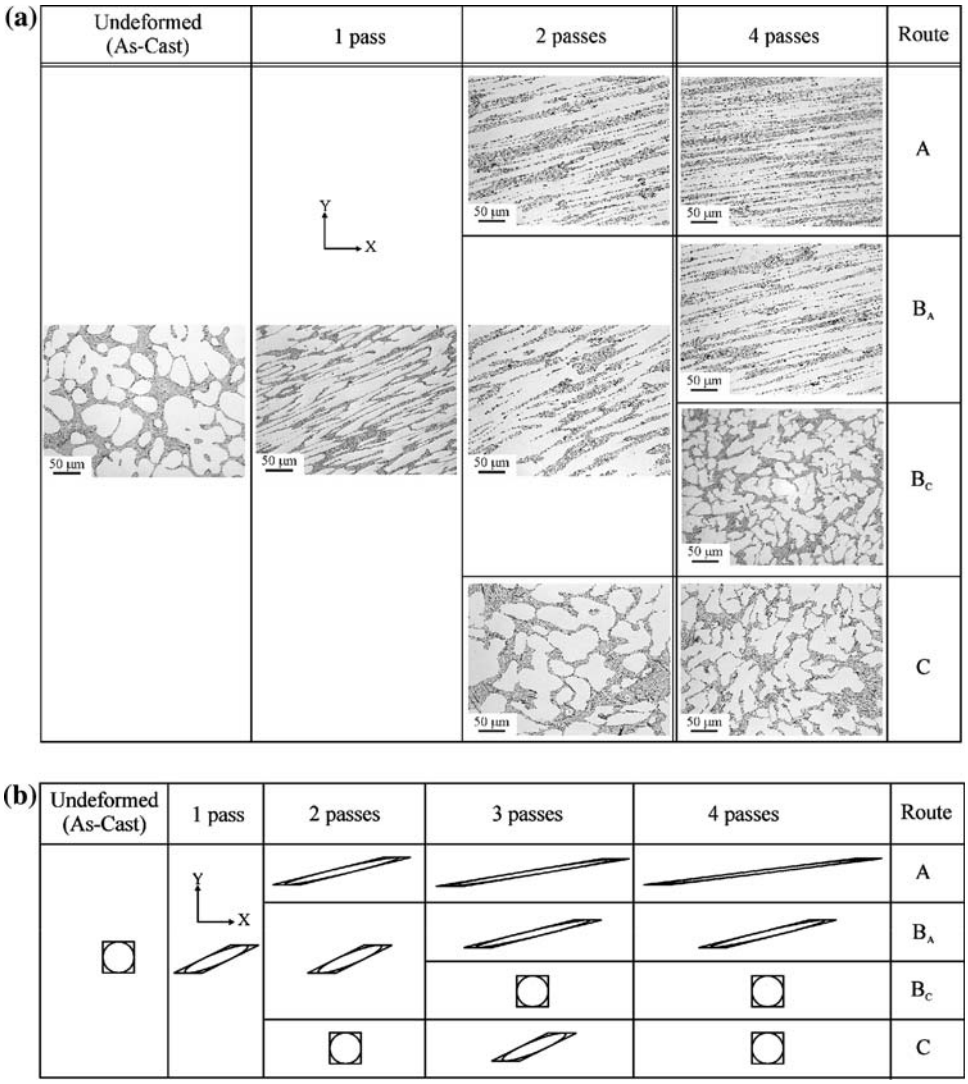

Fig. 3 (**a**) Flow plane optical microstructures of the as-cast material and material deformed to different number of passes by various routes. (**b**) Schematic illustrating the expected flow plane microstructures of an initial square element enclosing a circular element after deformation by various routes to up to four passes

The microstructures observed after ECAP processing through four passes by various routes are congruent with the geometrical shape change expected for an initially square element with an inscribed circle in the *X*–*Y* plane as the element is sheared following the various strain paths, as summarized in Fig. 3a and b. Here, the circle corresponds closely to the shapes of the primary Al dendrite cells in the alloy of the present work. By geometric analysis, it can be shown that the inclination of the long axis of the deformed ellipse in the flow plane (which is the inclination of the maximum principal strain axis) with the *X*-direction, β_N, is related to the apparent shear

Table 1 The values of γ_N for illustrating the flow plane microstructures observed during the first four passes by different routes

	γ_1	γ_2	γ_3	γ_4
Route A	2	4	6	8
Route B_A	2	2	4	4
Route B_C	2	2	0	0
Route C	2	0	2	0

strain in the flow plane imposed during ECAP, γ_N, after N passes[1] as [9]:

$$\beta_N = \tan^{-1}\left[\frac{1}{2\gamma_N}\left(\sqrt{(2+{\gamma_N}^2)^2-4}-{\gamma_N}^2\right)\right] \quad (1)$$

In order to obtain values for β_N through a sequence of ECAP passes, it is necessary to incorporate the appropriate value and sense of the γ_N through N passes for the route employed. Table 1 shows the idealized values of γ_N used to calculate the simulated flow plane microstructures for the first four passes by the different routes evaluated in this study. Table 2 summarizes the β_N values derived by incorporating values of γ_N from Table 1 in Eq. 1, again, for the various routes. For example, β_1 after one pass can be determined by using $\gamma_1 = 2$ in Eq. 1, giving a value of 22.5°. Without rotation between passes, the value of γ_2 is 4 for the second pass by route A, giving $\beta_2 = 13.3°$ from Eq. 1. In contrast, due to rotation of the billet upon the second pass in route B_C, the value of γ_2 is 0, and therefore, β_2 remains at 22.5°, thereby resulting in a flow plane microstructure essentially the same as that after one pass, while the total strain at this stage, γ_T, is now 4.

Likewise, the length of the minor axis of the deformed and elongated ellipse in the flow plane after processing by various routes to N passes, w_N, may be derived as [9]:

$$w_N = \frac{2d}{\sqrt{2[2+{\gamma_N}^2+\sqrt{(2+{\gamma_N}^2)^2-4}]}} \quad (2)$$

where d is the diameter of the circle prior to ECAP processing. The value of w_N obtained from Eq. 2 for the first four passes is listed in Table 3 for the values of γ_N from Table 1. These observations of shape change in the microstructure coupled with the theoretical analyses of shape change show that the microstructures in a two-phase alloy are strongly dependent on the ECAP processing routes and thus on the use of monotonic or redundant straining during SPD.

Of particular note is the lack of homogenization of second-phase particle distributions during SPD processing despite the large strains imparted to the material. The flow

[1] γ_N is different from the cumulative idealized shear strain, γ_T, experienced after N passes where $\gamma_T = 2N\cot(\varphi)$.

Table 2 Inclination of the major axis of the deformed ellipse (β) with the exit X-direction in the flow plane after ECAP processing

	1 Pass (β_1)	2 Passes (β_2)	3 Passes (β_3)	4 Passes (β_4)
Route A	22.5	13.3	9.2	7.0
Route B_A	22.5	22.5	13.3	13.3
Route B_C	22.5	22.5	[a]	[a]
Route C	22.5	[a]	22.5	[a]

[a] The microstructure becomes equiaxed at this stage

Table 3 Idealized length of the minor axis of the deformed ellipse in the flow plane distorted during ECAP processing of an initial undeformed circle having a diameter of 1 μm

	1 Pass (μm)	2 Passes (μm)	3 Passes (μm)	4 Passes (μm)
Route A	0.41	0.24	0.16	0.12
Route B_A	0.41	0.41	0.24	0.24
Route B_C	0.41	0.41	~1	~1
Route C	0.41	~1	0.41	~1

plane microstructure after route A suggests homogenization of the particle distribution, as does route B_A. The common feature of both these routes is the monotonic nature of the strain; however, examination of all three orthogonal planes in these as-processed billets would reveal distortion of the eutectic constituent but not redistribution of the particles [8]. Essentially, no homogenization of the particle distributions is apparent for redundant straining after every other pass by route C, and every four passes by route B_C, wherein the microstructures closely resemble that of the as-cast condition.

Figure 4 presents BSE images from the primary Al constituent of the Al–7wt%Si material after deformation to eight passes by either route A or B_C. The microstructure in the primary Al after eight passes by route A comprises of elongated dislocation structures, whereas the microstructure of the alloy subjected to same number of passes by route B_C consists of equiaxed dislocation structures that are similar in scale than those produced by route A. The dissimilarities between the microstructures after eight passes reflects different operative microstructure refinement mechanisms in processing by route A (monotonic shearing) in comparison to route B_C (redundant shearing). In route A, the progressive shearing of the primary Al dendrites causes their widths to become reduced. The apparent dislocation cell and subgrain structures that have formed in the primary Al are ~0.3 μm in width. When the primary Al dendrites are reduced in thickness to such a value, further straining would lead to pinching off of the elongated boundaries giving equiaxed structures by geometric-dynamic recrystallization (GDRX) [10]. In contrast, the appearance of microstructures resembling the as-cast microstructure after

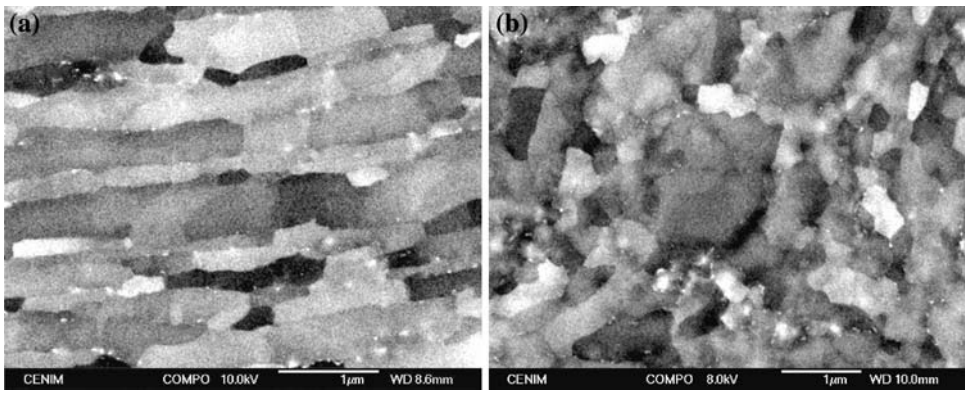

Fig. 4 BSE images from flow plane of Al–7wt%Si deformed to eight passes by (**a**) route A and (**b**) route B_C

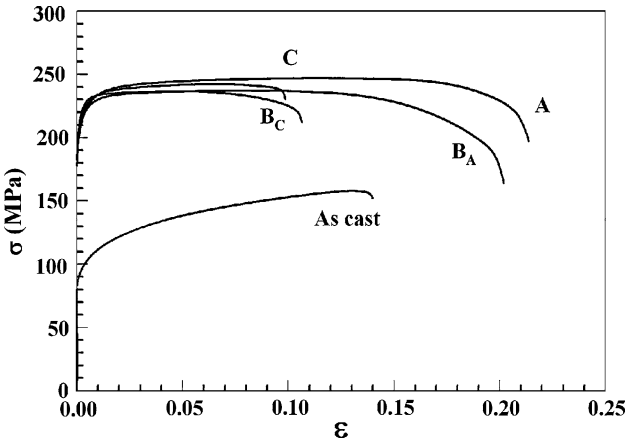

Fig. 5 True stress–true strain plots of as-cast as well as the alloy processed to eight passed by routes A, B_A, B_C and C [7]

every four passes in route B_C together with the presence of equiaxed dislocation structures in the primary Al dendrites is consistent with grain subdivision as the primary microstructure refinement mechanism.

The strain path employed during ECAP processes influences the mechanical properties as well through its effect on microstructure. True stress versus true strain plots from tensile tests of as-cast and alloy processed to eight passes by various routes are represented in Fig. 5. The tensile specimens were prepared having their tensile axes aligned with the *X*-direction (i.e., the die exit channel direction). The yield and ultimate strengths of the material deformed to eight passes by various routes is nearly the same, reflecting the equal degrees of strain hardening due to total equivalent cumulative strains for all cases. However, the degree of homogenization, as a consequence of monotonic versus redundant straining, affects the ductility of the deformed material. Processing by monotonic routes (e.g., routes A and B_A) enhances the ductility through distribution of particles into elongated, fibrous stringers aligned with the tensile direction. In contrast, the essential lack of homogenization of second-phase particle distributions after processing by redundant routes (C and B_C) results in a ready path for crack propagation through the eutectic constituent.

Conclusions

As-cast Al–7wt%Si hypoeutectic alloy billets were subjected to large strain deformation by ECAP employing routes: A, B_A, B_C, and C. From the flow plane microstructures, it is readily apparent that routes A and B_A involve monotonic shearing, while routes C and B_C involve redundant shearing after every two or four passes, respectively. The eutectic constituent in the Al–7wt%Si is a marker to delineate the effects of the processing routes and its shape change is congruent with that expected of an initial spherical element deformed by idealized ECAP processing. Furthermore, the microstructure refinement mechanisms may include geometrical dynamic recrystallization in monotonic shearing routes and grain subdivision in redundant shearing routes. The microstructures in the flow plane after monotonic shearing suggests homogenization of the eutectic constituents through a progressive decrease in the widths of the primary Al dendritic cells, while redundant straining results in microstructure resembling the as-cast microstructure with no homogenization after two and four passes in routes C and B_C, respectively. The apparent homogenization of particles during monotonic shearing reflects only the distortion of the eutectic constituent but not redistribution of particles, as is evident in the examination of all three orthogonal planes in these as-processed billets [8]. While the strengths are similar after equal number of pressing operations by various routes due to imposition of equivalent strains, the degree of homogenization affects the ductility. Monotonic routes show enhanced ductility compared to the redundant strain routes for samples oriented with their tensile axis aligned with the *X*-direction.

Acknowledgements The authors acknowledge financial support from CICYT under program MAT2003/01172. J. García-Infanta

would like to express his thanks to the Spanish Ministry of Education and Science for providing an FPI fellowship number BES-2004-4865, and travel expenses. T. R. McNelley and S. Swaminathan acknowledge partial support for this work by the U.S. Air Force Office of Scientific Research under funding document no. F1ATA06058G001. S. Swaminathan acknowledges a U.S. National Research Council Fellowship.

References

1. Segal VM, Reznikov VI, Drobyshevskiy AE, Kopylov VI (1981) Russ Metall 1:115
2. Segal VM (2003) Mater Sci Eng A 345:36. doi:10.1016/S0921-5093(02)00258-7
3. Segal VM (1995) Mater Sci Eng A 197:157. doi:10.1016/0921-5093(95)09705-8
4. Furukawa M, Iwahashi Y, Horita Z, Nemoto M, Langdon TG (1998) Mater Sci Eng A 257:328. doi:10.1016/S0921-5093(98)00750-3
5. Iwahashi Y, Horita Z, Nemoto M, Langdon TG (1998) Acta Mater 46:3317. doi:10.1016/S1359-6454(97)00494-1
6. Gholinia A, Prangnell PB, Markushev MV (2000) Acta Mater 48:1115. doi:10.1016/S1359-6454(99)00388-2
7. García-Infanta JM, Zhilyaev AP, Cepeda-Jiménez CM, Ruano OA, Carreno F (2008) Scr Mater 58:138. doi:10.1016/j.scriptamat.2007.09.018
8. García-Infanta JM, Swaminathan S, Zhilyaev AP, Carreño F, Ruano OA, McNelley TR (2007) Mater Sci Eng A doi:10.1016/j.msea.2007.07.080
9. García-Infanta JM, Swaminathan S, Carreño F, Ruano OA, McNelley TR (2008) Scr Mater 58:17. doi:10.1016/j.scriptamat.2007.09.007
10. Humphreys FJ, Hatherly M (2004) Recrystallization and related annealing phenomena. Elsevier, Oxford